

Sustainable preparation and characterization of thermally stable and functional cellulose nanocrystals and nanofibrils via formic acid hydrolysis

Haishun Du^{1,2}, Chao Liu¹, Dong Wang³, Yuedong Zhang¹, Guang Yu¹, Chuanling Si², Bin Li^{1*}, Xindong Mu¹, Hui Peng¹

1) CAS Key Laboratory of Bio-based Material, Qingdao Institute of Bioenergy and Bioprocess Technology, Chinese Academy of Sciences, Qingdao 266101, China

2) Tianjin Key Laboratory of Pulp and Paper, College of Papermaking Science and Technology, Tianjin University of Science and Technology, Tianjin 300457, China

3) CHTC Helon Co. Ltd., Weifang 261100, China

*Corresponding authors: libin@qibebt.ac.cn

ABSTRACT

In this work, a sustainable method to prepare functional cellulose nanocrystals (CNCs) and cellulose nanofibrils (CNFs) using formic acid (FA) (a recoverable organic acid) was established. After FA hydrolysis, the obtained CNCs could be well dispersed in DMAC. Thus, the CNC products and fibrous cellulosic solid residue (FCSR) in DMAC could be easily separated by a conventional centrifugal process, and the collected FCSR could be further fibrillated to CNFs with relatively low-intensity mechanical fibrillation process. The isolated CNC products showed high crystallinity index (about 75%) and excellent thermal stability (with onset thermal degradation temperature of 325 °C). Both the resultant CNCs and CNFs showed better dispersibility in DMSO, DMF and DMAC respectively because of the introduction of ester groups on the surface of the products. The presence of surface ester groups could increase the interface compatibility of nanocelluloses with polymeric matrices and enable their applications in reinforcing polymeric matrix materials (e.g. the composite films like PHVB+CNFs).

Keywords: Cellulose nanocrystals; Cellulose nanofibrils; Formic acid hydrolysis; Sustainable process; CNF/PHBV nanocomposites

1. INTRODUCTION

For the past few years, nanocellulose mainly obtained from native lignocellulosic biomass, is drawing growing attention due to their unique properties such as high tensile strength and elastic modulus, high specific surface area, low density, reactive surfaces combined with biodegradability and renewability.¹ Because of their special intrinsic nanostructure and distinctive properties, nanocelluloses have broad application prospects such as reinforcing fillers, electroconductive materials, packaging materials, and biomedical materials.²⁻⁴

Nanocellulose isolated from plant cell wall can be divided into two main categories: cellulose nanocrystals (CNCs) and cellulose nanofibrils (CNFs), which are different in morphology.⁵ In general, CNCs are rigid rod-like particles of 10–30 nm in width and several hundred nanometers in length and are mostly crystalline in nature, while CNFs are flexible fiber-like with a diameter less than 100 nm and the length of 500 nm or even longer. CNFs are composed of both amorphous and crystalline domains. The typical method for the preparation of CNCs involves a key hydrolysis step with strong inorganic acids, such as sulphuric, hydrochloric, nitric, phosphoric acids or their mixtures.⁶ Strong acid hydrolysis is indeed a simple and time-saving method for the preparation of CNCs. However, certain issues such as harsh corrosion of equipment, severe environmental pollution, large water usage, and low production yield need to be well addressed.⁶ Recently, some

solid acids (e.g. phosphotungstic acid)⁷ or organic acids such as formic acid,^{6,8} oxalic acid and maleic acid⁹ were used to replace the mineral acids to manufacture CNCs, because these solid acids and organic acids can be easily recovered and causes less equipment corrosion.

Different from CNCs, CNFs were mainly obtained by mechanical treatment of cellulosic fibers, such as homogenization, micro-fluidization, grinding, cryo-crushing, and ultrasonication.¹⁰ However, mechanical fibrillation for CNF production is very energy intensive. Some pretreatment methods have been proposed to reduce the energy consumption in the mechanical deconstruction process, including enzymatic hydrolysis, TEMPO-mediated oxidation, carboxymethylation, and quaternization, among others.¹¹

In our previous work, CNCs were prepared by formic acid (FA) hydrolysis, the FA could be easily recovered with a high recovery rate of over 90%, and the hydrolysate could also be directly reused for 1-3 times.^{6,8} However, a mixture of particles with different sizes (i.e. incompletely hydrolyzed cellulose fiber, partially hydrolyzed microfibrils, microfibril bundles and CNCs) could be obtained during in the FA hydrolysis process. Thus, the as-prepared CNC products have a broad range of particle size distribution. In order to obtain CNCs with uniform particle size, herein we reported a novel separation method based on the dispersibility of CNCs in certain solvents (e.g. dimethylacetamide (DMAC)). After FA hydrolysis and centrifugal washing, the CNC products and fibrous

cellulosic solid residue (FCSR) in DMAC could be easily separated by a centrifugal process as the CNCs could be well dispersed in DMAC. The CNCs could be obtained in the supernatant, and the FCSR could be readily fibrillated to CNFs with relatively low-intensity high-pressure homogenization by using DMAC as dispersion medium. Finally, the resulting two types of functional nanocelluloses were used as reinforcing agent for the preparation of PHBV nanocomposite films and the reinforcing effects were compared.

2. EXPERIMENTAL

2.1 Materials

The bleached softwood kraft pulp (BSKP) was obtained from Mudanjiang Hengfeng Paper Co., Ltd., China, and the pulp samples contained $85.5 \pm 0.5\%$ cellulose, $14.7 \pm 0.2\%$ hemicellulose and less than 0.1% lignin. The sugar composition of the BSKP was: 85.52% glucose, 8.05% xylose, 1.64% arabinose, 4.59% mannose and 0.42% galactose. Poly (3-hydroxybutyrate-co-3-hydroxyvalerate) (PHBV, PN009, BASF, Germany) was purchased from Dansheng Sujiao Co., Ltd. (Shenzhen, China). Formic acid (FA, 88 wt%), anhydrous ferric chloride (FeCl_3), imethylformamide (DMF), dimethylacetamide (DMAC) and dimethylsulfoxide (DMSO) were purchased from Sinopham Chemical Reagent Co., Ltd. All chemicals were used as received without further purification.

2.2 Preparation of CNCs and CNFs

The details for preparing the CNCs by formic acid hydrolysis were given in our previous work.^{6,8} In this study, we used FeCl_3 as a catalyst and prolonged the hydrolysis time to acquire more complete hydrolysis of cellulose and obtain more CNC products. The overall flowchart of FA hydrolysis and mechanical fibrillation processes for the preparation of CNCs and CNFs is shown in Fig. 1. Briefly, 10 g BSKP (oven dry) and 1g anhydrous FeCl_3 were added to a 500-mL spherical flask with 300 mL FA. The mixture was magnetically stirred at 300 rpm for 12 h at 95°C . Upon completion, the flask with the mixture was cooled down to room temperature with running water, and the reaction mixture was centrifuged in a Himac-CR22G II high speed refrigerated centrifuge (Hitachi, Japan) at 5000 rpm for 5 min. The separated hydrolysate could also be directly reused for the hydrolysis for 1-3 times. Then, the FA in the spent hydrolysate was recovered by vacuum distillation. After distillation, the solid residue was dissolved in 500 mL distilled water, and the FeCl_3 can be recovered as $\text{Fe}(\text{OH})_3$ via precipitation reaction with ammonium hydroxide. After separation of the hydrolysate, the obtained white residue was washed by successive centrifugation at 5000 rpm with distilled water. After centrifugation, the supernatant was decanted and the sediment was washed again. The washing was repeated until the pH of supernatant was about 6.0. After that, the sediment was dispersed in DMAC and

subsequently centrifuged at 3500 rpm for 5 min. After centrifugal separation, the CNCs could be obtained in the supernatant. The FCSR suspension in DMAC with the concentration of 0.2 wt% was passed through a GYB40-10S high-pressure homogenizer (Shanghai donghua high pressure homogenizer factory, China) 3 times at 300 bar and 7 times at 600 bar, and then the CNFs were obtained without further separation steps. The FCSR could be completely fibrillated to CNFs in DMAC even with low energy input. The corresponding energy consumption was about 19.20 kWh/kg CNFs under the same homogenization conditions as reported by Delgado-Aguilar et al.¹²

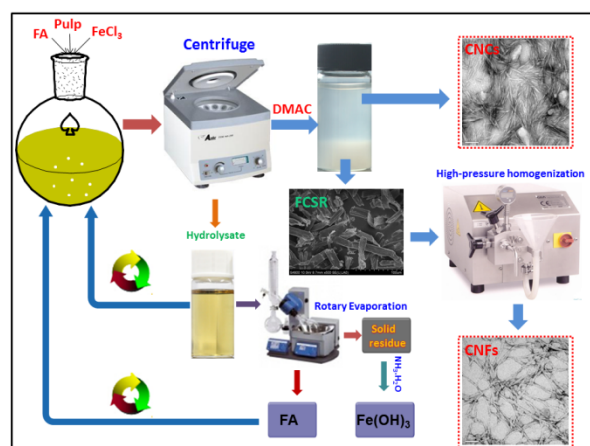


Fig. 1 Overall flowchart of formic acid hydrolysis and mechanical fibrillation processes for the preparation of CNCs and CNFs

2.3 Preparation of PHBV/CNCs or PHBV/CNFs nanocomposite films

PHBV/CNCs and PHBV/CNFs nanocomposite films were prepared using the solvent-casting method reported by Miao et al. with some modifications.¹³ Firstly, the concentration of CNCs or CNFs in DMAC was adjusted to 0.2 wt%. Then, 5 g of PHBV was added to 50 g of the CNC or CNF suspensions to prepare a nanocomposite film of 2% CNCs or CNFs content. The resulting mixture was stirred at 200 rpm at 80°C for 3 h. Subsequently, the mixture was cast on a flat glass sheet and let dry at 70°C overnight to form a film. Finally, the obtained film was further dried under vacuum at 40°C for 24 h to ensure that the solvent had completely evaporated.

2.4 The carbohydrate contents of supernatants

The carbohydrate contents of the hydrolysate were analyzed by high-performance anion-exchange chromatography with pulsed amperometric detection (HPAEC-PAD, Dionex ICS-3000, USA). The chromatography system and conditions used were identical to our previous work.⁶

2.5 Characterization of CNCs and CNFs

FTIR analyses of BSKP, CNC and CNF samples were carried out on a Thermo Nicolet FTIR spectrometer (Nicolet 6700, USA) in the wavenumber range of 400–4000 cm^{-1} with a resolution of 4 cm^{-1} . Before the analyses, the samples were freeze-dried and diluted to 1% by weight in KBr by grinding with a mortar and pestle. The X-ray diffraction (XRD) analysis of BSKP and the obtained nanocellulose were performed on a D8 Advanced Brüker diffract meter (Germany), and the crystallinity index (CrI) of each sample was calculated using the Segal equation.¹⁴ The morphology of BSKP and FCSR were observed by using a scanning electron microscope (Hitachi S-4800, Japan) at 5.0 kV. The samples were coated with gold under vacuum before observation. The morphology of CNCs and CNFs was observed using a TEM microscope (Hitachi H-7600, Japan). All the images were taken at 100 kV accelerating voltage. The dispersibility tests of CNC and CNF suspensions were conducted by centrifugation and solvent exchanging with DMSO, DMF and water, respectively, and the stability of the suspensions (2 mg/mL) was checked. All the samples were simultaneously treated by a VWR ultrasonic cleaner (45 kHz and 180 W) for 10 min and the pictures of samples were taken immediately after ultrasonic treatment and after standing for 1 day and 30 days, respectively. The re-dispersibility tests of CNC and CNF suspensions were conducted by adding freeze-dried samples to water, DMSO, DMF and DMAC and treated by a VWR ultrasonic cleaner (45 kHz and 180 W) for 10 min. Then, the stability of the suspensions (2 mg/mL) was checked. Thermal gravimetric analyses (TGA) of BSKP and nanocellulose samples were run on a thermo-gravimetric analyzer (TA Q600, Delaware, USA). The temperature elevated from room temperature to 600 °C at a heating rate of 10 °C/min under nitrogen (25 mL/min).

2.6 Characterization of PHBV/CNCs or PHBV/CNFs nanocomposite films

Table 1 Yields of CNCs, FCSR and degradation products in the hydrolysate^a

CNCs (%)	FCSR (%)	CF ^b (%)	Dis. glucose (%)	Dis. xylose (%)	Dis. arabinose (%)	Dis. mannose (%)	Dis. galactose (%)	Total (%)
12.46	63.98	5.23	2.86	7.92	1.25	4.37	0.38	98.45

^a The data represented the weight percentage based on the weight of starting BSKP.

^b CF: Cellulose formate (dissolved in hydrolysate).

3.2 Morphological analyses

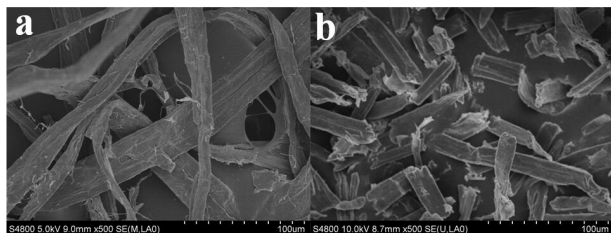


Fig. 2 SEM images of pulp (a) and FCSR (b)

Tensile strength of the PHBV/CNCs and PHBV/CNFs nanocomposite films were checked by universal testing machine with capacity of 50 N–10 kN load cell. The films were cut into pieces in the shape with width of 15 mm and total length of 100 mm. The tensile tests conducted in air using a 1 kN load cell at a crosshead speed of 50 mm/min, five measurements were made for each film and the data averaged to obtain a mean value.

3. RESULTS AND DISCUSSION

3.1 Preparation of CNCs and CNFs

Table 1 shows the yields of CNCs and FCSR as well as degradation products in hydrolysate. As indicated in Table 1, the CNC yield was low with the yield of approximately 12.5% due to insufficient hydrolysis, as the acidity of FA is weaker ($\text{pK}_a = 3.77$) than mineral acids such as sulfuric acid ($\text{pK}_a = -3.0$). The CNC yield was comparable with other results reported previously by using other organic acids (e.g. maleic or *p*-toluenesulfonic acid).⁷ The amount of dissolved glucose in the hydrolysate was small (2.86%, based on the mass of the starting material BSKP), while relatively large amounts of dissolved xylose (7.92%) and dissolved mannose (4.37%) were found in the hydrolysate. The results in Table 1 shows that only about 3.3% of the glucose in the BSKP but over 80% of the xylose and mannose were released from the original BSKP into the hydrolysate in the FA hydrolysis process, indicating that FA had a high selectivity in hydrolyzing hemicellulose.¹⁵ It is also worth mentioning that cellulose could react with FA at room temperature without using a catalyst.¹⁶ There was about 5% cellulose formate (CF) formed in the hydrolysate during the FA hydrolysis process. In addition, the yield of the CNCs or CNFs could be adjusted by tuning the hydrolysis conditions according to the requirement of the end products.

Shown in Fig. 2 are the SEM images of the original BSKP fibers and the FCSR after the FA hydrolysis. As can be seen, the length of the resultant FCSR decreased dramatically compared to the long BSKP fibers. Fig. 3 shows the TEM images of the CNCs and CNFs. As shown in Fig. 3a, relatively homogeneous CNCs could be obtained after the FA hydrolysis, and the width and length of the resultant CNCs were 5–20 nm and 50–200 nm, respectively. As shown in Fig. 3b, the FCSR could be successfully fibrillated to uniform CNFs via homogenization, and the width and length of the resultant F-CNF were found to be

5-20 nm and 300-1200 nm, respectively, by measuring 100 individual CNCs or CNFs with clearly identifiable ends.

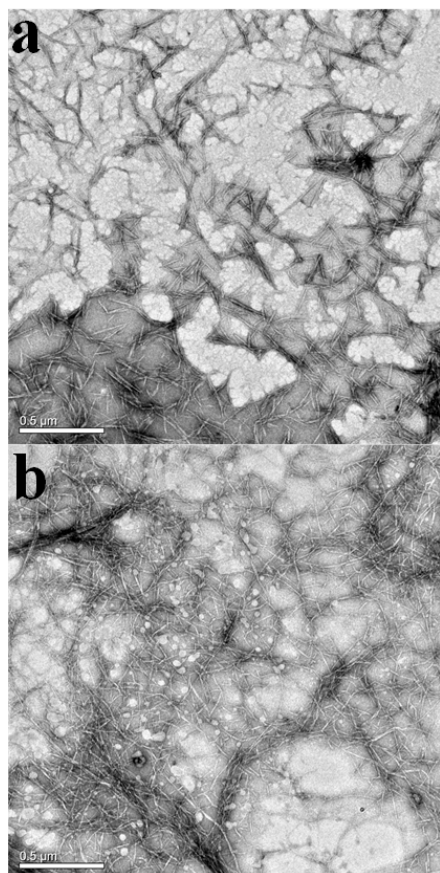


Fig. 3 TEM images of CNCs (a) and CNFs (b)

3.3 Surface chemical and crystalline structure of CNCs and CNFs

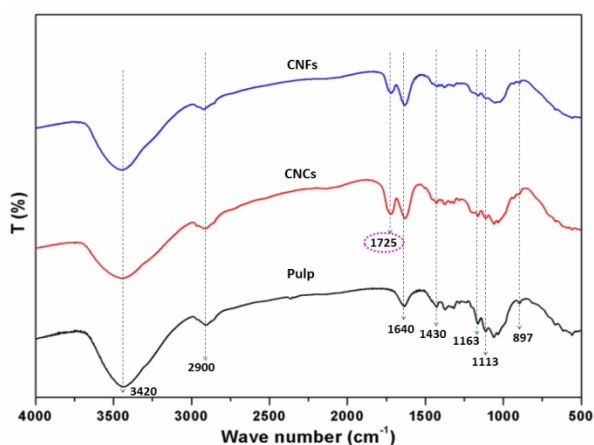


Fig. 4 FTIR spectra of pulp, CNCs and CNFs

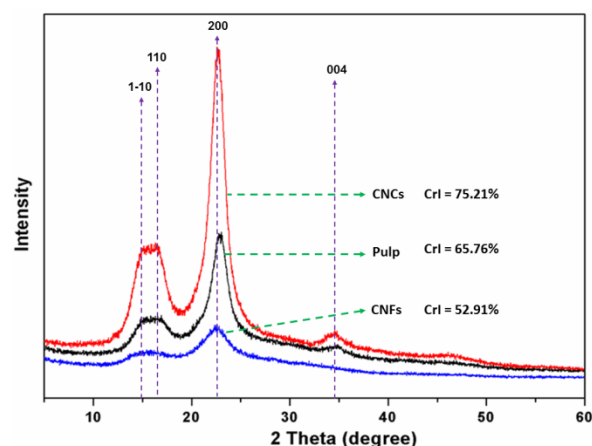


Fig. 5 XRD patterns of pulp, CNCs and CNFs

Fig. 4 shows the FTIR spectra of the CNCs and CNFs. It can be seen that a new strong absorption band at 1725 cm⁻¹ appeared in the spectrum of CNCs and CNFs while the other absorption bands were consistent with those for the BSKP. The new band at 1725 cm⁻¹ was ascribed to the C=O stretching of the ester groups newly formed in the CNCs and CNFs samples. During the FA hydrolysis, FA could react with cellulose, generating ester groups on the surface of the resulting nanocellulose.¹⁶

The XRD patterns of CNCs and CNFs are shown in Fig. 5. It can be seen that the XRD patterns of all the samples showed diffraction peaks at 2θ = 14.9°, 16.5°, 22.6° and 34.6°, corresponding to the (1-10), (110), (200) and (004) crystallographic planes of characteristic diffraction peaks of cellulose Iβ.¹⁷ The crystallinity index (CrI) calculated from the peak intensity was 65.76% for the original BSKP, and 75.21% for the CNCs. The CrI increased about 9.5% due to the hydrolysis of the hemicellulose and the amorphous regions of cellulose during the FA hydrolysis.⁶ However, the CrI of the CNFs clearly decreased, which was probably due to the damage of the crystalline domains of cellulose during the high-pressure homogenization process.¹⁸

3.4 Dispersibility and re-dispersibility studies

Fig. 6 illustrates the dispersibility of CNCs and CNFs in water, DMSO, DMF and DMAC, respectively. As shown in Fig. 6a, after ultrasonic treatment, both the CNCs and CNFs could be dispersed in water, DMSO, DMF and DMAC, respectively. The CNCs were not stable in water, but very stable in other 3 solvents. After 1 day standing, the CNCs dispersed in water started to flocculate, but remained well dispersion in the other 3 solvents. In contrast, the CNFs were well dispersed in all the four solvents. The seven CNCs and CNFs suspensions (except for the suspension of CNCs in water) remained stable for over a month at room temperature. The improved dispersibility of CNCs and CNFs in organic solvents probably due to the formation of ester groups on the surface of F-CNFs which in turn increased its compatibility in organic solvents.

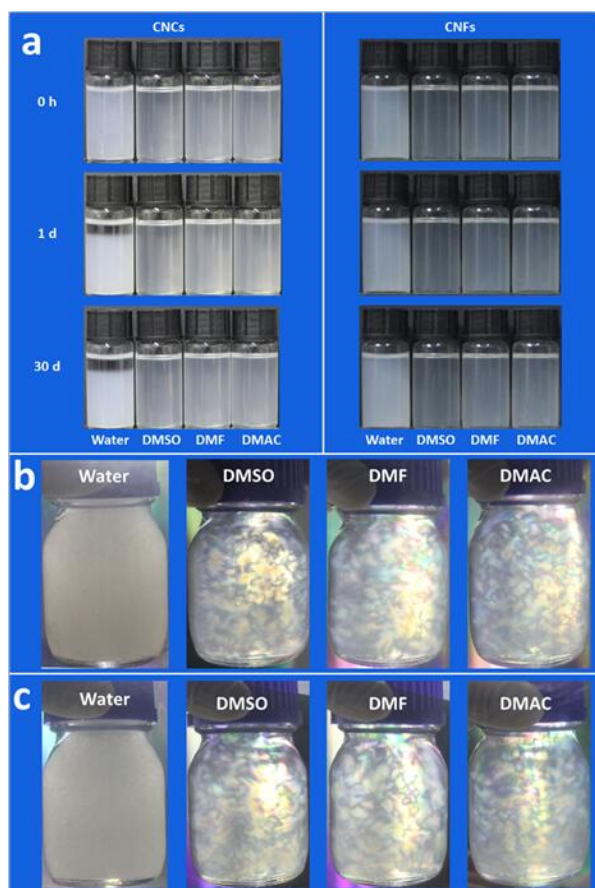


Fig. 6 Dispersibility of CNCs and CNFs in water, DMSO, DMF and DMAC (a), typical flow birefringence phenomena observed under polarized light for CNC (b) and re-dispersed CNCs (c) suspensions in water, DMSO, DMF and DMAC after ultrasonication

Fig. 6b gives the characteristic flow birefringence phenomena of CNCs in DMSO, DMF and DMAC when observed between two crossed linear polarizing films. It was worth mentioning that the freeze-dried CNCs could be easily dispersed in DMSO, DMF, and DMAC with retained flow birefringence (Fig. 6c). However, the flow birefringence phenomena could not be observed for the CNF suspensions, and the freeze-dried CNFs could not be well dispersed in the four solvents, probably due to the lower degree of esterification.

3.5 Thermal gravimetric analysis

As shown in Fig. 7, the thermal stability of the original BSKP fibers, CNCs and CNFs could be sorted in an ascending order: CNFs < BSKP < CNCs. The onset decomposition temperature of the CNFs, BSKP and CNCs were about 282, 321 and 325 °C, respectively. The maximum decomposition temperature of the CNFs, BSKP and CNCs and were about 305, 351 and 356 °C, respectively. The increase of thermal stability of the CNCs compared to original BSKP fibers was probably due to the removal of amorphous materials (e.g. disordered regions of

cellulose and hemicellulose) after the FA hydrolysis.⁶ The obvious decrease in the thermal stability of the CNFs probably due to the damages in the crystal region of cellulose during the homogenization process, as indicated by the XRD results in Fig. 5.

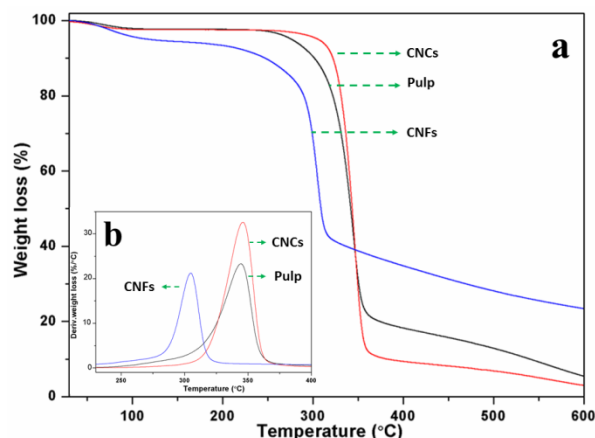


Fig. 7 TG (a) and DTG (b) curves of pulp, CNCs and CNFs

3.6 Reinforcing effects on PHBV nanocomposite films

As shown in Fig. 8, the PHBV/CNCs and PHBV/CNFs nanocomposite films maintained the transparency properties of PHBV matrix, indicating the CNCs and CNFs had good compatibility with the polymer matrix without nanofiller aggregation. Table 2 shows the mechanical behaviors of neat PHBV, PHBV/CNCs and PHBV/CNFs nanocomposite films, illustrating that the tensile strength and Young's modulus effectively increased after the incorporation of CNCs or CNFs, along with slight reduction in elongation at break was found for the nanocomposite films. The tensile strength increased 38% for the PHBV/CNFs nanocomposite film compared to the pure PHBV. This improvement was clearly higher than that achieved by the enhancement of CNCs, due to the fact that the CNFs had a network structure and a much higher length to width ratio for better reinforcing effect on the tensile strength, compared with the rod-like CNCs. However, the rod-like CNCs exhibited better reinforcing effect on the Young's modulus than the CNFs.

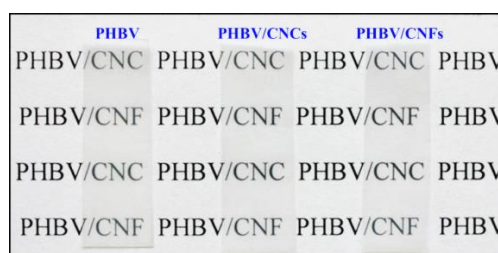


Fig. 8 Images to show the transparency of the PHBV, PHBV/CNCs and PHBV/CNFs nanocomposite films

Table 2 Tensile strength, Young's modulus and elongation at break for neat PHBV, PHBV/CNCs and PHBV/CNFs nanocomposite films

Samples	Tensile strength (MPa)	Young's modulus (MPa)	Elongation at break (%)
PHBV	13.56±0.35	60.98±1.21	922.94 ±2.17
PHBV/CNCs	17.47±0.47	83.46±1.35	841.68 ±1.81
PHBV/CNFs	18.68±0.39	73.38±0.83	875.99 ±1.67

4. CONCLUSIONS

This study demonstrated a sustainable method for the preparation of functional CNCs and CNFs by FA hydrolysis followed by mechanical fibrillation. The CNCs had high crystallinity and excellent thermal stability. Both the CNCs and CNFs could be easily dispersed in DMSO, DMF and DMAC due to the introduction of ester groups on the surface of the CNCs and CNFs. Both types of nanocelluloses exhibited significant reinforcing effect on the PHBV nanocomposite films for high quality food packaging applications.

ACKNOWLEDGMENTS

This work was financially supported by the National Natural Science Foundation of China (contract grant numbers: 21306261, 31470609, and 25106240) and Primary Research and Development Plan of Shandong Province (contract grant numbers: 2016GGX104003, and 2016CYJS07A02).

REFERENCES

1. Moon R J., Martini A., Nairn J., Simonsen J., Youngblood J. Cellulose nanomaterials review: structure, properties and nanocomposites. *Chemical Society Reviews*, 2011, 40, 3941-3994. doi: 10.1039/c0cs00108b
2. Zhu H., Luo W., Ciesielski P N., Fang Z., Zhu J., Henriksson G., Himmel M E., Hu L. Wood-Derived Materials for Green Electronics, Biological Devices, and Energy Applications. *Chemical Reviews*, 2016, 116, 9305-9374. doi: 10.1021/acs.chemrev.6b00225
3. Hunan Liang, Xiao Hu. A quick review of the applications of nano crystalline cellulose in wastewater treatment. *Journal of Bioresources and Bioproducts*, 2016, 1(4), 199-204.
4. Qinzhi Li, Bing Wei, Yan Xue, Yangbing Wen, Jing Li. Improving the physical properties of nano-cellulose through chemical grafting for potential use in enhancing oil recovery. *Journal of Bioresources and Bioproducts*, 2016, 1(4), 186-191.
5. Liu C., Li B., Du H., Lv D., Zhang Y., Yu G., Mu X., Peng H. Properties of nanocellulose isolated from corncob residue using sulfuric acid, formic acid, oxidative and mechanical methods. *Carbohydrate Polymers*, 2016, 151, 716-724. doi: 10.1016/j.carbpol.2016.06.025
6. Du H., Liu C., Mu X., Gong W., Lv D., Hong Y., Si C., Li B. Preparation and characterization of thermally stable cellulose nanocrystals via a sustainable approach of FeCl₃-catalyzed formic acid hydrolysis. *Cellulose*, 2016, 23, 2389-2407. doi: 10.1007/s10570-016-0963-5
7. Liu Y., Wang H., Yu G., Yu Q., Li B., Mu X. A novel approach for the preparation of nanocrystalline cellulose by using phosphotungstic acid. *Carbohydrate Polymers*, 2014, 110, 415-422. doi: 10.1016/j.carbpol.2014.04.040
8. Li B., Xu W., Kronlund D., Maattanen A., Liu J., Smatt J H., Peltonen J., Willfor S., Mu X., Xu C. Cellulose nanocrystals prepared via formic acid hydrolysis followed by TEMPO-mediated oxidation. *Carbohydrate Polymers*, 2015, 133, 605-612. doi: 10.1016/j.carbpol.2015.07.033
9. Chen L., Zhu J., Baez C., Kitin P., Elder T. Highly thermal-stable and functional cellulose nanocrystals and nanofibrils produced using fully recyclable organic acids. *Green Chemistry*, 2016, 18, 3835-3843. doi: 10.1039/c6gc00687f
10. Jonooobi M., Oladi R., Davoudpour Y., Oksman K., Dufresne A., Hamzeh Y., Davoodi R. Different preparation methods and properties of nanostructured cellulose from various natural resources and residues: a review. *Cellulose*, 2015, 22, 935-969. doi: 10.1007/s10570-015-0551-0
11. Nechyporchuk O., Belgacem M N., Bras J. Production of cellulose nanofibrils: A review of recent advances. *Industrial Crops and Products*, 2016, 93, 2-25. doi: 10.1016/j.indcrop.2016.02.016
12. Delgado-Aguilar M., Gonzalez I., Tarres Q., Alcala M., Angels Pelach M., Mutje Pere. Approaching a low-cost production of cellulose nanofibers for papermaking applications. *Bioresources*, 2015, 10, 5345-5355. doi: 10.15376/biores.10.3.5345-5355
13. Miao J., Yu Y., Jiang Z., Zhang L. One-pot preparation of hydrophobic cellulose nanocrystals in an ionic liquid. *Cellulose*, 2016, 23, 1209-1219. doi: 10.1007/s10570-016-0864-7
14. Segal L., Creely J J., Martin A E., Jr., Conrad C M. An empirical method for estimating the degree of crystallinity of native cellulose using the X-ray diffractometer. *Textile Research Journal*, 1959, 29, 786-794. doi: 10.1177/004051755902901003
15. Yu G., Li B., Liu C., Zhang Y., Wang H., Mu X. Fractionation of the main components of corn stover by formic acid and enzymatic saccharification of solid residue. *Industrial Crops and Products*, 2013, 50, 750-757. doi: 10.1016/j.indcrop.2013.08.053
16. Fujimoto T., Takahashi S I., Tsuji M., Miyamoto T., Inagaki H. Reaction of cellulose with formic acid and stability of cellulose formate. *Journal of Polymer Science Part C-Polymer Letters*, 1986, 24, 495-501. doi: 10.1002/pol.1986.140241002
17. Li Q., Renneckar S. Supramolecular structure characterization of molecularly thin cellulose I nanoparticles. *Biomacromolecules*, 2011, 12, 650-659. doi: 10.1021/bm101315y
18. Saelee K., Yingkamhaeng N., Nimchua T., Sukyai P. An environmentally friendly xylanase-assisted pretreatment for cellulose nanofibrils isolation from sugarcane bagasse by high-pressure homogenization. *Industrial Crops and Products*, 2016, 82, 149-160. doi: 10.1016/j.indcrop.2015.11.064